Inflammation-induced repression of tumor suppressor miR-7 in gastric tumor cells

著者	Kong Dan, Piao Ying-Shi, Yamashita Satoshi, Oshima Hiroko, Oguma Keisuke, Fushida Sachio, Fujimura Takashi, Minamoto Toshinari, Seno Hiroshi, Yamada Yoichi, Satou Kenji, Ushijima Toshikazu, Ishikawa Tomo-o, Oshima Masanobu
journal or publication title	Oncogene
volume	31
number	35
page range	3949-3960
year	2012-08-30
URL	http://hdl.handle.net/2297/32470

doi: 10.1038/onc.2011.558

Inflammation-induced repression of tumor suppressor miR-7 in gastric tumor cells

Dan Kong[1,8], Ying-Shi Piao[1,7,8], Satoshi Yamashita[2], Hiroko Oshima[1], Keisuke Oguma[1], Sachio Fushida[3], Takashi Fujimura[3], Toshinari Minamoto[4], Hiroshi Seno[5], Yoichi Yamada[6], Kenji Satou[6], Toshikazu Ushijima[2], Tomo-o Ishikawa[1], Masanobu Oshima[1]

[1]Division of Genetics, Cancer Research Institute, Kanazawa University, Kanazawa 920-1192, Japan; [2]Division of Epigenomics, National Cancer Center Research Institute, Tokyo 104-0045, Japan; [3]Gastroenterologic Surgery, Kanazawa University Hospital, Kanazawa Japan, 920-8641, Japan; [4]Division of Translational and Clinical Oncology, Cancer Research Institute, Kanazawa University, Kanazawa 920-0934, Japan; [5]Department of Gastroenterology and Hepatology, Kyoto University Graduate School of Medicine, 606-8507, Japan; [6]Faculty of Electrical and Computer Engineering, Institute of Science and Engineering, Kanazawa University, Kanazawa 920-1192, Japan.
[7]Present address: Department of Pathophysiology, Medical College, Yanbian University, Yanji City, 133002, China

Correspondence: Professor M. Oshima, Division of Genetics, Cancer Research Institute, Kanazawa University, Kakuma-machi, Kanazawa, 920-1192, Japan.
E-mail address: oshimam@kenroku.kanazawa-u.ac.jp

[8]These authors contributed equally to this work.

Running Title: Repression of miR-7 by inflammation

Key words: miR-7, gastric cancer, inflammation, macrophages

Word count: 4,487 excluding abstract, references, and Figure legends

ABSTRACT

Inflammation plays an important role in cancer development through a variety of mechanisms. It has been shown that dysregulation of microRNAs (miRNAs) that function as oncogenes or tumor suppressors contributes to tumorigenesis. However, the relationship between inflammation and cancer-related miRNA expression in tumorigenesis has not yet fully understood. Using *K19-C2mE* and *Gan* mouse models that develop gastritis and gastritis-associated tumors, respectively, we found that 21 miRNAs were upregulated, and that 29 miRNAs were downregulated in gastric tumors in an inflammation-dependent manner. Among these miRNAs, the expression of miR-7, a possible tumor suppressor, significantly decreased in both gastritis and gastric tumors. Moreover, expression of miR-7 in human gastric cancer was inversely correlated with the levels of IL-1β and TNF-α, suggesting that miR-7 downregulation is related to the severity of inflammatory responses. In the normal mouse stomach, miR-7 expression was at a basal level in undifferentiated gastric epithelial cells, and was induced during differentiation. Moreover, transfection of a miR-7 precursor into gastric cancer cells suppressed cell proliferation and soft agar colony formation. These results suggest that suppression of miR-7 expression is important for maintaining the undifferentiated status of gastric epithelial cells, and thus contributes to gastric tumorigenesis. Although epigenetic changes were not found in the CpG islands around miR-7-1 of gastritis and gastric tumor cells, we found that activated macrophage-derived small molecule(s) (< 3 kDa) are responsible for miR-7 repression in gastric cancer cells. Furthermore, the miR-7 expression level significantly decreased in the inflamed gastric mucosa of

Helicobacter-infected mice, while it increased in the stomach of germfree *K19-C2mE* and *Gan* mice where the inflammatory responses were suppressed. Taken together, these results indicate that downregulation of tumor suppressor miR-7 is a novel mechanism by which the inflammatory response promotes gastric tumorigenesis.

Introduction

It has been established that inflammatory responses contribute to cancer development through a variety of mechanisms (Coussens and Werb, 2002). The expression of cyclooxygenase-2 (COX-2), a rate-limiting enzyme for prostaglandin biosynthesis, plays an important role in both inflammation and cancer (Wang and DuBois, 2010). Using genetic mouse models, we previously demonstrated that induction of COX-2 and its downstream product, prostaglandin E_2 (PGE_2), is required for gastrointestinal tumorigenesis (Sonoshita *et al.*, 2001; Oshima *et al*., 2006). The COX-2/PGE_2 pathway, together with a bacterial infection, induces inflammatory responses in the stomach through the recruitment of macrophages, which promotes gastric tumorigenesis (Oshima *et al*., 2011). However, it remains to be fully elucidated precisely how such inflammatory responses contribute to the promotion of gastric tumors.

MicroRNAs (miRNAs) are a class of single-stranded small noncoding RNAs that regulate gene expression by post-transcriptional interference of the specific mRNAs (Ambros, 2004; Bartel, 2004). Through their regulation of cancer-related gene expression, miRNAs can function as either oncogenes or tumor suppressors (Esquela-Kerscher and Slack, 2006; Ventura and Jacks, 2009). The dysregulation of miRNAs in cancer has been shown to be associated with genomic/epigenetic alterations or transcriptional/post-transcriptional mechanisms (Di Leva and Croce, 2010). Moreover, expression of several miRNAs, including oncogenic miRNAs, has been shown to be induced by inflammatory responses (Sonkoly and Pivarcsi, 2011). For example, miR-155 is induced in macrophages by NF-κB, interferon (IFN)-β, or Toll-like receptor signaling

(Tili *et al*., 2007; O'Connell *et al*., 2007), while miR-21 is induced by Stat3, a transcription factor activated by IL-6 (Ilipoulos *et al*., 2010). On the other hand, the mechanism responsible for the downregulation of tumor suppressor miRNA expression in the inflammatory microenvironment has not been fully understood.

We herein examined the expression of miRNAs in mouse models of gastritis and gastric tumors, which were developed in *K19-C2mE* mice and *Gan* mice, respectively (Oshima *et al*., 2004; Oshima *et al*., 2006). We found the expression level of miR-7 to significantly decrease in gastric tumors in an inflammation-dependent manner. It has been shown that miR-7 plays a tumor suppressor role in several cancers, including glioblastoma, breast cancer, and lung cancer (Kefas *et al*., 2008; Reddy *et al*., 2008; Webster *et al*., 2009; Jiang *et al*., 2010; Saydam *et al*., 2011). In this manuscript, we demonstrate that miR-7 is induced during the differentiation of normal gastric epithelial cells, and it also plays a tumor suppressor role in the stomach. These results suggest that downregulation of tumor suppressor miR-7 is one of the tumor-promoting mechanisms underlying the role of inflammation in gastric tumorigenesis.

Results

Inflammation-dependent dysregulation of miRNAs in gastric tumors

To examine whether miRNA expression is dysregulated in gastric tumors by inflammatory responses, we examined the miRNA expression profiles in wild-type mouse stomachs from the *K19-C2mE* mouse gastritis and the *Gan* mouse gastric tumors by a microarray analysis. In *Gan* mouse gastric tumors, 50 miRNAs were upregulated (>2.0 fold), while 42 miRNAs were downregulated (< 0.5 fold) compared with the wild-type mouse stomach level (Figure 1a and Supplementary Table 1). Notably, 21 and 29 miRNAs showed upregulation or downregulation, respectively, in both gastritis and gastric tumors. It is therefore possible that dysregulation of these miRNAs is caused by inflammatory responses.

We confirmed the results of the microarray analysis by real-time RT-PCR. Ten miRNAs randomly selected from the upregulated and downregulated miRNAs (Figure 1a, *boxed*) showed the same dysregulation pattern in both gastritis and gastric tumors (Figure 1b). Importantly, miR-155 and miR-21, which function as oncogenes (Volinia *et al*., 2006) were upregulated, whereas miR-145 and miR-7, which function as tumor suppressors (Sachdeva *et al*., 2009; Kefas *et al*., 2008), were downregulated in both gastritis and gastric tumors (Figure 1a, b). This suggests that inflammation can induce not only upregulation of oncogenic miRNAs, but also downregulation of tumor suppressor miRNAs.

We next picked up 74 miRNAs that were not dysregulated in *K19-C2mE* gastritis compared with wild-type normal stomach (Supplementary Table 2). Among them, 3 miRNAs were upregulated in *Gan* mouse tumors compared with *K19-C2mE* gastritis tissue samples (> 2.0 fold), while 3 miRNA were downregulated (< 0.5 fold) (Figure 1c). It is

possible that expression of these miRNAs is dysregulated by carcinogenesis-specific mechanisms.

Induction of miR-7 during differentiation of gastric epithelial cells

We further examined the expression of miR-7, because its role(s) in the normal stomach and gastric cancer have never been examined. Gastric glands were isolated from the stomachs of the respective mouse models, and the miR-7 expression was examined by real-time RT-PCR. Notably, the miR-7 levels were significantly lower in the epithelial cells of *K19-C2mE* gastritis tissues and *Gan* mouse tumors compared with the wild-type mouse stomach (Figure 2a), indicating that miR-7 is predominantly expressed in epithelial cells in an inflammation-dependent manner.

When the primary cultured gastric epithelial cells were passaged and maintained for 6 days, the cell morphology appeared to be differentiated, with enlarged and mucin-containing cytoplasm (Figure 2b). Consistently, the expression of differentiation markers, *Muc6* and *Muc5AC*, was elevated on day 6, whereas the expression of the Wnt target gene, *Sox9*, decreased (Figure 2c). These results indicate that the cultured gastric epithelial cells underwent differentiation through passage and 6 days culture. Importantly, the miR-7 expression level increased significantly on day 6, to 6.5-fold the level observed on day 2.

We next examined the miR-7 level in the stomach during development. The expression level of miR-7 in the stomach increased significantly in the 14-day-old and adult mice, to more than 6-fold of that in E15 embryos (Figure 2d). Conversely, expression of

CD44, one of the Wnt target genes, decreased significantly during development. We confirmed by an immunohistochemistry that most epithelial cells in the gastric mucosa were Ki-67 positive on days 0 and 7, while the proliferating cells were limited to the gland neck on day 14 and in adult mice (Figure 2e). Accordingly, the ratio of undifferentiated epithelial cells decreased during development. Taken together, these results indicate that miR-7 expression is induced in gastric epithelial cells during differentiation.

Tumor suppressor role of miR-7 in gastric cancer development

We next examined the miR-7 levels in human gastric cancers by real-time RT-PCR. The expression of miR-7 was downregulated in 18 out of 28 human gastric cancer tissue samples (64%) compared with paired non-tumor stomach tissue samples (Figure 3a), suggesting that miR-7 has a tumor suppressor role in a subpopulation of gastric cancers. We next examined expression level of IL-1β and TNF-α, major proinflammatory cytokines, and compared them with the miR-7 level. Importantly, expression levels of miR-7 were inversely correlated to those of IL-1β or TNF-α, suggesting that downregulation of miR-7 is related to the severity of inflammatory responses (Figure 3b). We also found that miR-7 was markedly downregulated in 4 out of 9 gastric cancer cells lines (Figure 3c).

To examine the tumor suppressor role of miR-7 in gastric tumorigenesis, we transfected the precursor of miR-7, pre-miR-7, into AZ-521 and Kato-III gastric cancer cells and examined their proliferation and soft agar colony formation. We confirmed that pre-miR-7 transfection into the reporter vector-transfected cells resulted in a significant decrease in luciferase activity, indicating an increase of mature miR-7 level (Supplementary

Figure 1). Transfection of pre-miR-7 significantly decreased cell proliferation in both cell lines compared with control vector-transfected cells (Figure 3d). Moreover, pre-miR-7 transfection significantly suppressed the soft agar colony formation in both cell lines (Figure 3e and f). These results strongly suggest that miR-7 has a tumor suppressor role in gastric cancer development.

Repression of miR-7 in gastric cancer cells by macrophage-derived factor(s)

We detected primary (pri)-miR-7-1, pri-miR-7-2 and pri-miR-7b in the mouse normal stomach by real-time RT-PCR (Supplementary Figure 2), suggesting that mature miR-7 is processed from all these primary miR-7 in the normal gastric mucosa. MiR-7-1 is located in the intron of the *Hnrnpk* gene, and a CpG island is found in the promoter region of *Hnrnpk* (Supplementary Figure 3a). On the other hand, we could not determine CpG islands that regulate the transcription of miR-7-2 and miR-7b. We thus examined DNA methylation in the CpG islands in the *Hnrnpk* promoter region. Notably, DNA methylation levels in *K19-C2mE* gastritis and *Gan* mouse tumor tissues were not increased compared with the wild-type mouse stomach (Supplementary Figure 3a). Consistently, DNA methylation was not detected in the promoter region of the *HNRNPK* gene in the human gastric cancer tissues (Figure 4a). We also examined the trimethylation of histone H3 at lysine 27 (H3K27me3) in the upstream CpG islands of *Hnrnpk*. However, the H3K27me3 level was not increased in the mouse gastritis and gastric tumors compared with the wild-type stomach (Figure 4b). These results indicate that DNA methylation and trimethylation of H3K27 are not involved in the downregulation of miR-7-1. Moreover,

the genomic region including miR-7-1 was not deleted in human gastric cancer cells (Supplementary Figure 3b), suggesting that miR-7 downregulation in gastric cancer is not caused by genomic deletion.

We next examined whether activated macrophages play a role in downregulation of miR-7, because the major source of proinflammatory cytokines in gastric tumors are macrophages (Oshima *et al*., 2004; Oshima *et al*., 2011). To monitor the miR-7 activity, reporter vector-transfected cells were used. We confirmed that the luciferase activity was increased significantly when miR-7 inhibitor was transfected into the reporter vector-transfected Kato-III cells (Supplementary Figure 1c), indicating that the luciferase reporter system was working. Reporter cells were then treated with the conditioned medium of LPS-stimulated RAW264 cells [CM(+)] or unstimulated RAW264 cells [CM(-)]. Importantly, the luciferase activity increased significantly when cells were stimulated with CM(+), while the luciferase activity was not changed in the control vector-transfected cells (Figure 4c). Similar results were obtained when CM(+) and CM(-) were prepared using mouse intraperitoneal macrophages. These results indicate that activated macrophage-derived factor(s) caused the miR-7 downregulation in gastric cancer cells.

To identify the macrophage-derived factor(s) that suppress miR-7 expression, the reporter cells were stimulated with TNF-α, IL-1β, IL-6 or PGE_2. However, none of these factors caused an increase in the luciferase activity (Supplementary Figure 4). We thus fractionated the CM(+) by ultrafiltration, and separated by molecular weight. Interestingly, a CM(+) fraction of < 3 kDa significantly increased the luciferase activity to a similar level as that induced by whole CM(+), whereas the other CM(+) fractions did not (Figure 4d).

Moreover, the luciferase activity was still increased when CM(+) was prepared under co-treatment of RAW264 cells with LPS and a COX-2 inhibitor, celecoxib. We confirmed the decreased level of miR-7 by real-time RT-PCR in the CM(+)- or CM(+) fraction < 3 kDa-treated AZ521 cells (Figure 4e). These results indicate that small molecule(s) (< 3kDa) derived from activated macrophages are responsible for the miR-7 repression in gastric cancer cells, and that such small molecule(s) are expressed in activated macrophages in a COX-2/PGE_2-independent manner.

Downregulation of miR-7 in the stomach by inflammatory responses

We next examined whether inflammatory responses are responsible for the miR-7 downregulation in the stomach using different mouse models. The stomachs of wild-type mice were infected with *Helicobacter felis*, and submucosal inflammatory infiltration and mucosal macrophage accumulation were confirmed at 20 weeks after the infection (Figure 5a, b). Notably, the miR-7 expression level was significantly decreased in the *H. felis*-infected inflamed gastric mucosa (Figure 5c).

We recently showed that inflammatory responses and macrophage infiltration were suppressed in the *K19-C2mE* mouse gastritis and *Gan* mouse tumors when mice were maintained under germfree conditions (Figure 5d, and Oshima *et al*., 2011). Notably, the miR-7 expression levels were increased significantly in germfree *K19-C2mE* and *Gan* mice compared with the levels of SPF mice (Figure 5e). These *in vivo* experiments suggest that inflammatory responses are responsible for the miR-7 downregulation in the stomach, although further genetic studies are required to examine the role of macrophages in miR-7

downregulation.

Inflammation-dependent upregulation of miR-7 target genes in gastric tumors

The epidermal growth factor receptor (EGFR) mRNA is one of the miR-7 target genes (Kefas *et al*., 2008; Webster *et al*., 2009). We thus examined the EGFR expression levels in the pre-miR-7-transfected Kato-III and AZ521 gastric cancer cells. As expected, EGFR expression level was decreased significantly by pre-miR-7 transfection in both cell lines (Figure 6a), suggesting that suppression of EGFR expression is one of the tumor suppressor mechanisms of miR-7 against gastric cancer development.

To identify novel miR-7 target genes that are upregulated in the inflammatory microenvironment, we searched for putative miR-7 target genes from the upregulated gene set in both *K19-C2mE* mouse gastritis and *Gan* mouse gastric tumors using the results of the microarray analyses (Itadani *et al*., 2009). We found that the *Lphn2*, *Basp1*, and *Mafg* genes have conserved miR-7 target sequences in their 3' UTR in both mouse and human mRNAs (Figure 6b). Notably, expression of these genes was significantly increased not only in the *K19-C2mE* mouse gastritis and *Gan* mouse tumors, but also in *K19-Nog/C2mE* mouse gastric hamartomas (Figure 6c). The gastric mucosa and tumors in these strains are inflamed as a result of the induction of the COX-2/PGE_2 pathway (Oshima *et al*., 2004, 2006, and 2009), suggesting that downregulation of miR-7 in inflammatory lesions is involved in upregulation of these genes. Notably, transfection of pre-miR-7 into Kato-III cells resulted in a significant decrease of *LPHN2*, *BASP1*, and *MAFG* expression (Figure 6d). Moreover, we constructed luciferase reporter plasmids that contained the 3' UTR

fragment of the putative miR-7 target genes, and transfected these vectors into Kato-III cells. Consistent with the real-time RT-PCR results, the luciferase activities of the reporter vector-transfected cells decreased significantly when cells were co-transfected with pre-miR-7 (Figure 6e). Taken together, these results indicate that these three genes are miR-7 targets.

Finally, we examined expression of *LPHN2*, *BASP1*, and *MAFG* in human gastric cancers by real-time RT-PCR and compared their expression with the miR-7 expression levels. We found that the expression levels of miR-7 and *LPHN2*, *BASP1*, *MAFG* were inversely correlated (Figure 6f). Accordingly, it is possible that inflammation causes induction of these genes in human gastric cancers through downregulation of miR-7, which may contribute to gastric tumorigenesis, although this will need to be investigated in future studies.

Discussion

It has been shown that miR-155 and miR-21, which function as oncogenes, are induced by inflammatory pathways, providing a link between inflammation and cancer (Tili *et al*., 2007; O'Connell *et al*., 2007; Iliopoulos *et al*., 2010). Consistently, we found inflammation-dependent induction of miR-155 and miR-21 in mouse gastric tumors. On the other hand, miR-145 and miR-7, which function as tumor suppressors, are downregulated in both the mouse gastritis and gastric tumor tissues. Moreover, we found that the miR-7 levels are inversely correlated with the levels of proinflammatory cytokines, suggesting that the severity of inflammatory response is related to miR-7 downregulation. It is therefore possible that inflammation can promote tumorigenesis both by the upregulation of oncogenic miRNAs and by the downregulation of tumor suppressor miRNAs, possibly through different mechanisms. Such alterations of cancer-related miRNA expression likely link inflammation and cancer.

It has been reported that miR-7 plays a tumor suppressor role in a variety of cancers including brain tumors, breast cancer, and lung cancer (Kefas *et al*., 2008; Reddy *et al*., 2008; Webster *et al*., 2009), and we herein showed that miR-7 also functions as a tumor suppressor in gastric cancer. Interestingly, in the normal stomach, miR-7 expression is induced during the differentiation of gastric epithelial cells, suggesting a role of miR-7 in the regulation of epithelial cell differentiation. It has also been reported that miR-7 expression is induced during the differentiation of intestinal epithelial cells (Nguyen *et al*., 2010) and cortical neurons (Chen *et al*., 2010). These results collectively suggest that miR-7 plays a role in regulating cell differentiation in a variety of organs. It is therefore

conceivable that the suppression of miR-7 expression is required for the maintenance of the undifferentiated status of stem or progenitor cells in these organs.

The present results suggest the possibility that inflammation suppresses epithelial cell differentiation through repression of miR-7. It is not surprising that the inflammatory response suppresses cell differentiation and enhances proliferation when regeneration is required in injured tissues. It has also been shown that a disruption of toll-like receptor signaling causes an impairment of tissue repair by intestinal epithelial cells (Rakoff-Nahoum *et al*., 2004). Moreover, activated macrophages are important niche components for intestinal epithelial progenitors in regenerative responses (Pull *et al*., 2005). Therefore, it is conceivable that downregulation of miR-7 leads to suppression of differentiation, inducing the proliferation of undifferentiated epithelial cells in the inflammatory microenvironment.

Although several target genes of miR-7 have been identified, it is still unclear how miR-7 regulates differentiation. EGFR is one of the important miR-7 target genes, and is at least partially responsible for its tumor suppressor role (Kefas *et al*., 2008). Moreover, p21-activated kinase 1, Raf1, and the insulin-like growth factor 1 receptor have also been identified as miR-7 target genes that are upregulated in cancer cells (Reddy *et al*., 2008; Webster *et al*., 2009; Jiang *et al*., 2010). Although most of these gene products contribute to cancer cell proliferation, we believe that miR-7 inhibits expression of other factors that play a role in the maintenance of the undifferentiated status of epithelial cells. In the present study, we identified three novel miR-7 target genes that are upregulated in gastric cancers in an inflammation-dependent manner. LPHN2 is a G protein-coupled receptor

that binds α-latrotoxin (Ichtchenko *et al*., 1999), while BASP1 is implicated in neurite outgrowth (Korshunova *et al*., 2008). MAFG is one of the small Maf proteins that are important for antioxidant responses (Katsuoka et al., 2005). Although it remains to be investigated, it is of interest to examine whether these molecules play any role in the differentiation or tumorigenesis of gastric epithelial cells.

We examined the mechanisms responsible for the miR-7 downregulation in gastric tumor cells. *Helicobacter pylori* infection induces chronic gastritis, resulting in induction of DNA methylation (Niwa *et al*., 2010). The expression of miR-34b/c is suppressed by DNA methylation in *H. pylori*-associated gastric cancer cells (Suzuki *et al*., 2010). Moreover, H3K27me3 leads to tumor-suppressor gene silencing in cancer (Kondo *et al*., 2008). However, we showed that downregulation of miR-7 is not caused by genomic deletion nor by epigenetic mechanisms, but through stimulation by macrophage-derived factor(s). Several mechanisms for the regulation of miR-7 expression have been reported. For example, miR-7 transcription is directly induced by HoxD10 (Reddy *et al*., 2008) or c-Myc (Chou *et al*., 2010). Splicing factor SF2/ASF binds the pri-miR-7 to enhance its cleavage by Drosha (Wu *et al*., 2010). Accordingly, it is conceivable that macrophage-derived molecule(s) directly downregulate the miR-7 expression or indirectly suppress the miR-7 expression through modulation of these regulation systems. The identification of responsible macrophage-derived molecule(s) will provide a novel mechanism by which macrophages promote tumorigenesis.

In conclusion, we showed that inflammation simultaneously induces the upregulation of oncogenic miRNAs and the downregulation of tumor suppressor miRNAs, which

promote tumorigenesis. The expression of miR-7 is induced during differentiation of gastric epithelial cells, suggesting a role for miR-7 in the regulation of epithelial cell differentiation. Accordingly, it is possible that the downregulation of miR-7 contributes to suppression of differentiation, resulting in the promotion of gastric tumorigenesis. Moreover, small molecule(s) expressed by activated macrophages are responsible for miR-7 repression, providing a link between inflammation and cancer. Therefore, miR-7 may be useful for devising a new preventive or therapeutic strategy against gastric cancer through the induction of cancer cell differentiation.

Materials and methods

Mouse models

Construction of *K19-C2mE* and *Gan* (*K19-Wnt1/C2mE*) mice was described previously (Oshima *et al*., 2004, and 2006). Briefly, *K19-C2mE* mice express *Ptgs2* and *Ptges* in gastric epithelial cells, whereas *Gan* mice express *Ptgs2*, *Ptges* and *Wnt1*. For the expression analyses, the *K19-C2mE* mouse gastritis and *Gan* mouse gastric tumor samples, and wild-type mouse stomach tissues were obtained at 30~40 weeks of age. Germfree mouse colonies were constructed as described previously (Oshima *et al*., 2011), and the histology and miR-7 expression were examined at 55 weeks of age (n=5). *Helicobacter felis* (ATCC 49179) were inoculated at 10^8/mouse into the wild-type mice at 6~8 weeks of age, and the histology and miRNA expression were examined at 20 weeks after infection (n=6). All animal experiments were carried out according to a protocol approved by the Committee on Animal Experimentation of Kanazawa University.

Microarray analysis

Total RNA was extracted from mouse stomachs (n=3) using ISOGEN (Nippon Gene, Tokyo, Japan), pooled with the same genotype mouse RNAs, labeled with Cy3, and hybridized to Mouse miRNA microarray Rel. 12.0 (Agilent Technologies, Santa Clara, CA). The raw data were normalized using the GeneSpring GX software program (Agilent Technologies), and the expression levels of miRNAs in gastritis and gastric tumor tissues were compared with those in the wild-type mouse stomach. Transcripts with low signals (less than three-fold of the background level) were not used for further analyses.

Expression of miRNAs was further examined by real-time RT-PCR using RNA samples independently prepared from a different set of wild-type, *K19-C2mE* and *Gan* mice (n=5 for each genotype).

The results of cDNA microarray data sets of *K19-C2mE*, *Gan*, and *K19-Nog/C2mE* mice were deposited into the Gene Expression Omnibus (GEO), as accession number GSE16902 (Itadani et al., 2009), and were searched for the presence of novel miR-7 target genes using the TargetScan 5.1 program (http://www.targetscan.org).

Real-time RT-PCR

Paired gastric cancer and non-tumor stomach tissue samples were obtained from 28 patients during surgery at Kanazawa University Hospital, Japan. Fresh frozen tissues were used for the expression analyses. Clinicopathological data of patients are shown in Supplementary Table 3. Human normal gastric epithelial cells were prepared by isolating the gastric glands from normal stomach tissues (n=4) as described previously (Cheng *et al*., 1984). Approval for this project was obtained from the Kanazawa University Medical Ethics Committee, and written informed consent was obtained before specimen collection. Mouse stomachs were obtained from E15 wild-type mouse embryos, and day 0, day 7, day 14 and adult mice (n=3 for each). Total RNAs were extracted from the tissues or cells using ISOGEN (Nippon Gene), and the cDNAs for miRNAs and mRNAs were constructed using QuantiMir RT Kit (System Bioscience, Mountain View, CA) and the PrimeScript RT reagent Kit (Takara, Tokyo, Japan), respectively. Real-time RT-PCR was performed using SYBR Premix Ex TaqII (Takara, Tokyo, Japan) and Stratagene Mx3000P (Agilent

Technologies). Sno202 and U44 were used as endogenous miRNA controls for mice and humans, respectively, whereas β-actin was used for endogenous mRNA control. The primer sequences for the miRNAs are shown in Supplementary Table 4. The primers for mRNAs were purchased from Takara (Tokyo, Japan).

Cell culture experiments

Mouse glandular stomachs were treated with 0.1% collagenase for 30 min at 37^{o}C, followed by centrifugation at 20 *g* for 3 min to isolate gastric glands. For the primary culture, isolated gastric glands were digested with trypsin and seeded on collagen-coated dishes as described (Oshima *et al*., 2004). On day 2, the primary cultured cells were treated with 10mM EDTA-PBS and passaged. The primary cultured cells on day 2 (P0) and day 6 (P1) were used for the expression analysis. Human gastric cancer cell lines, AGS (ATCC), AZ521, MKN74, MKN45, NUGC4, HCT-111-TC, SH-10-TC (RIKEN BioResource Center, Tsukuba, Japan), Kato-III, and MKN7 (Cell Resource Center for Biomedical Research, Tohoku University, Japan) were used in this study.

The pre-miR miRNA-7 (Pre-miR-7), pre-miR negative control (Pre-miR-NC) and anti-miR-7 inhibitor (Ambion, Austin, TX) were used for transfection. The cell proliferation rate was measured using the Cell Counting Kit-8 (Dojindo, Kumamoto, Japan). For the soft agar colony formation assay, cells were suspended in culture medium with 0.33% agar, and seeded in a 6-well plate. After 21 days of culture, soft agar was stained with Giemsa solution (Wako, Osaka, Japan).

Histological and immunohistochemical analyses

Tissues were fixed in 4% paraformaldehyde, embedded and sectioned at 4-μm thickness. The sections were stained with H&E. Antibodies against Ki-67 (DakoCytomation, Carpentria, CA) and F4/80 (Serotec, Oxford, UK) were used as the primary antibodies. Immunostaining signals were visualized using the Vectastain Elite Kit (Vector Laboratories, Burlingame, CA), and the MOM kit (Vector Laboratories) was used to minimize the background staining signals.

Methylation-specific PCR (MSP) analysis

The methylation status of miR-7-1 in human gastric cancer and non-tumor tissues was examined by MSP analysis as described (Yamashita *et al*., 2008). The MSP was performed with a primer set specific for the methylated or unmethylated sequence (Me or Un set in Supplementary Table 4). DNA methylated by SssI methylase (New England Biolabs) and DNA amplified by a GenomiPhi DNA amplification kit (GE Healthcare Bio-Science) were used as methylated and unmethylated controls, respectively.

Chromatin immunoprecipitation (ChIP) analyses

Histone modifications were examined by ChIP assay as described (Yamashita *et al*., 2008; Takeshima *et al*., 2009). Briefly, gastric epithelial cells of wild-type, *K19-C2mE*, and *Gan* mice (n=3 for each genotype) were cross-linked with 1% formaldehyde, and sheared chromatin by Bioruptor UCD-250 (Cosmo Bio, Tokyo, Japan). The samples were incubated with an antibody against H3K27me3 (07-449, Millipore, Billerica, MA), and

genomic DNA samples were used for the quantitative ChIP-PCR analyses. The primer set was designed for the upstream CpG islands of miR-7-1 (Supplementary Table 4).

Luciferase reporter assay

Construction of the miR-7 luciferase reporter vector (miR-7 Luc) and control vector (control Luc) are shown in Supplementary Figure 1. Luciferase reporter vectors for the *LPHN2*, *BASP1*, and *MAFG* genes were constructed by subcloning 3' UTR fragments of the respective human genes into the pGL3 plasmid (Promega, Madison, WI). PCR primer sequences for cloning 3' UTR of the respective genes and amplified fragment lengths are indicated in Supplementary Table 4. The luciferase activity was measured using a Luciferase Assay System (Promega) and the levels were normalized to the total protein levels detected by Pierce 660 nm Protein Assay (Thermo Scientific, Yokohama, Japan). RAW264 cells (RIKEN BioResource Center) and mouse intraperitoneal macrophages were stimulated with 10 ng/ml of LPS (Sigma) for 24 hours and the conditioned medium was collected as CM(+). The conditioned medium of the unstimulated macrophages was collected as CM(-). The conditioned medium of the LPS-stimulated and COX-2 inhibitor celecoxib (Pfizer)-treated (10 μM) RAW264 cells was collected as CM(+/coxib). The CM(+) was fractionated by ultrafiltration using Centricon Plus-70 (Millipore, Billerica, MA) to prepare CM(+) >100 kDa, 30~100 kDa, 3~30 kDa, and < 3 kDa. Cells were stimulated with CM at a 50% concentration.

Western blotting analysis

Cells were transfected with pre-miR-7 or the pre-miR-NC, lysed at 24 hours after transfection, and 10 μg of protein were separated in 7.5% SDS-polyacrylamide gels. An antibody against EGFR (Cell Signaling Technology, Danvers, MA) was used as the primary antibody. Anti-β-actin (Sigma) was used as an internal control. The ECL detection system (GE Healthcare, Buckinghamshire, UK) was used to detect the signals, and the band intensities were quantified using the ImageJ application (NIH).

Statistical analysis

The data were analyzed by the unpaired *t*-test using the Microsoft Excel software program (Microsoft). A value of $p < 0.05$ was considered to be statistically significant.

Conflict of interest

The authors declare no conflict of interest.

Acknowledgement

We thank Manami Watanabe for her excellent technical assistance. This work was supported by Grants-in-Aid from the Ministry of Education, Culture, Sports, Science and Technology of Japan, and the Ministry of Health, Labour and Welfare of Japan.

References

Ambros V. (2004) The functions of animal microRNAs. *Nature* **431**: 350-355.

Bartel DP. (2004) MicroRNAs: Genomics, biogenesis, mechanism, and function. *Cell* **116**: 281-297.

Chen H, Shalom-Feuerstein R, Riley J, Zhang SD, Tucci P, Agostini M *et al*. (2010) miR-7 and miR-214 are specifically expressed during neuroblastoma differentiation, cortical development and embryonic stem cells differentiation, and control neurite outgrowth in vitro. *Biochem Biophys Res Commun* **394**: 921-927.

Cheng H, Bjerknes M, Amar J. (1984) Methods for the determination of epithelial cell kinetic parameters of human colonic epithelium isolated from surgical and biopsy. *Gastroenterology* **86**: 78-85.

Chou YT, Lin HH, Lien YC, Wang YH, Hong CF, Kao YR *et al*. (2010) EGFR promotes lung tumorigenesis by activating miR-7 through a Ras/ERK/Myc pathway that targets the Ets2 transcriptional repressor ERF. *Cancer Res* **70**: 8822-8831.

Coussens LM, Werb Z. (2002) Inflammation and cancer. *Nature* **420**: 860-867.

Di Leva G, Croce CM. (2010) Roles of small RNAs in tumor formation. *Trends Mol Med* **16**: 257-267.

Esquela-Kerscher A, Slack FJ. (2006) Oncomirs-microRNAs with a role in cancer. *Nat Rev Cance*r **6**: 259-269.

Ichtchenko K, Bittner MA, Krasnoperov V, Little AR, Chepurny O, Holz RW et al. (1999) A novel ubiquitously expressed α-latrotoxin receptor is a member of the CIRL family of G-protein-coupled receptors. *J Biol Chem* **274**: 5491-5498.

Iliopoulos D, Jaeger SA, Hirsch HA, Bulyk ML, Struhl K. (2010) STAT3 activation of miR-21 and miR-181b-1 via PTEN and CYLD are part of the epigenetic switch linking inflammation to cancer. *Mol Cell* **39**: 493-506.

Itadani H, Oshima H, Oshima M, Kotani H. (2009) Mouse gastric tumor models with prostaglandin E_2 pathway activation show similar gene expression profiles to intestinal-type human gastric cancer. *BMC Genomics* **10**: 615.

Jiang L, Liu X, Chen Z, Jin Y, Heidbreder CE, Kolokythas A *et al*. (2010) MicroRNA-7 targets IGF1R (insulin-like growth factor 1 receptor) in tongue squamous cell carcinoma cells. *Biochem J* **432**: 199-205.

Katsuoka F, Motohashi H, Ishii T, Aburatani H, Engel JD, Yamamoto M. (2005) Genetic evidence that small maf proteins are essential for the activation of antioxidant response element-dependent genes. *Mol Cell Biol* **25**: 8044-8051.

Kefas B, Godlewski J, Comeau L, Li Y, Abounader R, Hawkinson M *et al*. (2008) microRNA-7 inhibits the epidermal growth factor receptor and the Akt pathway and is down-regulated in glioblastoma. *Cancer Res* **68**: 3566-3572.

Kondo Y, Shen L, Cheng AS, Ahmed S, Boumber Y, Charo C *et al*. (2008) Gene silencing in cancer by histone H3 lysine 27 trimethylation independent of promoter methylation. *Nat Genet* **40**: 741-750.

Korshunova I, Caroni P, Kolkova K, Berezin V, Bock E, Walmod PS. (2008) Characterization of BASP-1 mediated neurite outgrowth. *J Neurosci Res* **86**: 2201-2213.

Niwa T, Tsukamoto T, Toyoda T, Mori A, Tanaka H, Maekita T *et al*. (2010) Inflammatory processes triggered by *Helicobacter pylori* infection cause aberrant DNA methylation in

gastric epithelial cells. *Cancer Res* **70**: 1430-1440.

Nguyen HT, Dalmasso G, Yan Y, Laroui H, Dahan S, Mayer L *et al*. (2010) MicroRNA-7 modulates CD98 expression during intestinal epithelial cell differentiation. *J Biol Chem* **285**: 1479-1489.

O'Connell RM, Taganov KD, Boldin MP, Cheng G, Baltimore D. (2007) MicroRNA-155 is induced during the macrophage inflammatory response. *Proc Natl Acad Sci USA* **104**: 1604-1609.

Oshima H, Oshima M, Inaba K, Taketo MM. (2004) Hyperplastic gastric tumors induced by activated macrophages in COX-2/mPGES-1 transgenic mice. *EMBO J* **23**: 1669-1678.

Oshima H, Matsunaga A, Fujimura T, Tsukamoto T, Taketo MM, Oshima M. (2006) Carcinogeniesis in mouse stomach by simultaneous activation of the Wnt signaling and prostaglandin E_2 pathway. *Gastroenterology* **131**: 1086-1095.

Oshima H, Itadani H, Kotani H, Taketo MM, Oshima M. (2009) Induction of prostaglandin E_2 pathway promotes gastric hamartoma development with suppression of bone morphogenetic protein signaling. *Cancer Res* **69**: 2729-2733.

Oshima H, Hioki K, Popivanova BK, Oguma K, van Rooijen N, Ishikawa TO *et al*. (2011) Prostaglandin E_2 signaling and bacterial infection recruit tumor-promoting macrophages to mouse gastric tumors. *Gastroenterology* **140**: 596-607, 2011

Pull SL, Doherty JM, Mills JC, Gordon JI, Stappenbeck TS. (2005) Activated macrophages are an adaptive element of the colonic epithelial progenitor niche necessary for regenerative responses to injury. *Proc Natl Acad Sci USA* **102**: 99-104.

Rakoff-Nahoum S, Paglino J, Eslami-Varzaneh F, Edberg S, Medzhitov R. (2004) Recognition of commensal microflora by Toll-like receptors is required for intestinal homeostasis. *Cell* **118**: 229-241.

Reddy SD, Ohshiro K, Rayala SK, Kumar R. (2008) MicroRNA-7, a homeobox D10 target, inhibits p21-activated kinase 1 and regulates its functions. *Cancer Res* **68**: 8195-8200.

Sachdeva M, Zhu S, Wu F, Wu H, Walia V, Kumar S et al. (2009) p53 represses c-Myc through induction of the tumor suppressor miR-145. *Proc Natl Acad Sci USA* **106**: 3207-3212.

Saydam O, Senol O, Wurdinger T, Mizrak A, Ozdener GB, Stemmer-Rachamimov AO *et al*. (2011) miRNA-7 attenuation in Schwannoma tumors stimulates growth by upregulating three oncogenic signaling pathways. *Cancer Res* **71**: 852-861.

Sonkoly E, Pivarcsi A. (2011) MicroRNAs in inflammation and response to injuries induced by environmental pollution. Mutat Res Feb 15 [Epub ahead of print]

Sonoshita M, Takaku K, Sasaki N, Sugimoto Y, Ushikubi F, Narumiya S *et al*. (2001) Acceleration of intestinal polyposis through prostaglandin receptor EP2 in $Apc^{\Delta 716}$ knockout mice. *Nat Med* **7**: 1048-1051.

Suzuki H, Yamamoto E, Nojima M, Kai M, Yamano H, Yoshikawa K *et al*. (2010) Methylation-associated silencing of microRNA-34b/c in gastric cancer and its involvement in an epigenetic field defect. *Carcinogenesis* **31**: 2066-2073.

Takeshima H, Yamashita S, Shimazu T, Niwa T, Ushijima T. (2009) The presence of RNA polymerase II, active or stalled, predicts epigenetic fate of promoter CpG islands. *Genome Res* **19**: 1974-1982.

Tili E, Michaille JJ, Cimino A, Costinean S, Dumitru CD, Adair B *et al*. (2007) Modulation of miR-155 and miR-125b levels following lipopolysaccharide/TNF-α stimulation and their possible roles in regulating the response to endotoxin shock. *J Immunol* **179**: 5082-5089.

Ventura A, Jacks T. (2009) MicroRNAs and cancer: Short RNAs go a long way. *Cell* **136**: 586-591.

Volinia S, Calin GA, Liu CG, Ambs S, Cimmino A, Petrocca F *et al*. (2006) A microRNA expression signature of human solid tumors defines cancer gene targets. *Proc Natl Acad Sci USA* **103**: 2257-2261.

Wang D, DuBois RN. (2010) Eicosanoids and cancer. *Nat Rev Cancer* **10**: 181-193.

Webster RJ, Giles KM, Price KJ, Zhang PM, Mattick JS, Leedman PJ. (2009) Regulation of epidermal growth factor receptor signaling in human cancer cells by microRNA-7. *J Biol Chem* **284**: 5731-5741.

Wu H, Sun S, Tu K, Gao Y, Xie B, Krainer AR *et al*. (2010) A splicing-independent function of SF2/ASF in microRNA processing. *Mol Cell* **38**: 67-77.

Yamashita S, Takahashi S, McDonell N, Watanabe N, Niwa T, Hosoya K *et al*. (2008) Methylation silencing of transforming growth factor-β receptor type II in rat prostate cancers. *Cancer Res* **68**: 2112-2121.

Figure legends

Figure 1. Inflammation-dependent dysregulation of miRNA expression in mouse gastric tumors. (a) Venn diagrams of the miRNAs that were upregulated (> 2.0) and downregulated (< 0.5) in *Gan* mouse gastric tumors and/or *K19-C2mE* mouse gastritis samples as determined by the microarray analysis are shown. The miRNAs listed in boxes were upregulated (*left*) or downregulated (*right*) in both the gastric tumor and gastritis tissue samples. (b) The relative expression levels of selected miRNAs (indicated in **bold** in the list) for *K19-C2mE* mouse gastritis (*blue bars*) and *Gan* mouse gastric tumors (*red bars*) compared to the wild-type levels examined by real-time RT-PCR are shown as the log10 ratios. $*p < 0.05$ versus the wild-type level. The expression levels of miRNAs were normalized to the Sno202 level. (c) The miRNA levels in *Gan* mouse tumors relative to those in *K19-C2mE* gastritis tissues examined by the microarray analysis are shown. Red and blue bars indicate upregulated (> 2.0) and downregulated (< 0.5) miRNAs, respectively, in *Gan* mouse tumors.

Figure 2. The induction of miR-7 expression in the differentiated gastric epithelial cells. (a) A representative photograph of isolated gastric glands from wild-type mice (*top*, arrows). The expression levels of miR-7 in the isolated gastric glands of *K19-C2mE* and *Gan* mice relative to the wild-type level are shown (mean ± s.d.) (*bottom*). $*p < 0.05$. (b) Representative photographs of the primary cultured gastric epithelial cells on day 2 (passage 0: *P0*) and day 6 (passage 1: *P1*) (original magnification, ×100). Arrows in P1 indicate mucin-containing enlarged cells on day 6. (c) The levels of *Muc6*, *Muc5AC*, and

Sox9 mRNA and miR-7 in the primary cultured gastric epithelial cells on day 6 (*closed bars*) relative to the levels on day 2 (*gray bars*) are shown (mean ± s.d.). *$p < 0.05$ versus the day 2 level. (d) The expression levels of miR-7 (*gray bars*) and CD44 (*open bars*) in the stomach at the indicated ages relative to the levels in E15 embryos are shown (mean ± s.d.). *$p < 0.05$ versus the E15 level. The expression levels of miR-7 were normalized to the Sno202 level. (e) Representative photographs of Ki-67 immunostaining in the glandular stomach of mice at the indicated ages. Asterisks indicate proliferative zones. Scale bars indicate 50 μm.

Figure 3. The tumor suppressor roles of miR-7 in gastric cancer cells. (a) The relative miR-7 expression levels in the human gastric cancer tissue samples to the level of non-tumor stomach tissue samples are shown as the Log10 ratios. The indicated numbers correspond to the patient ID in the clinicopathological data (Supplementary Table 3). (b) Comparison of the relative expression levels of miR-7 and IL-1β (*left*) or TNF-α (*right*) in gastric cancer tissues to the non-tumor stomach tissue levels in each patient is shown. Red and blue lines indicate that the expression of miR-7 was increased (> 1.0) and decreased (<1.0) in the gastric cancers, respectively. (c) The relative expression levels of miR-7 in gastric cancer cell lines compared to the mean level in the human normal gastric epithelial cells are shown as the Log10 ratios. The expression levels of miR-7 were normalized to that of U44. (d) The proliferation of control (*gray bars*) and pre-miR-7-transfected (*closed bars*) AZ521 cells and Kato-III cells at the indicated culture days are shown (mean ± s.d.). *$p < 0.05$. (e) Representative photographs of soft agar colonies in 6 well plates

showing the pre-miR-NC- (*left*) and pre-miR-7-transfected (*right*) Kato-III cells. (f) The mean numbers of soft agar colonies larger than the indicated diameters in each well of 6-well plate of control (*gray bars*) and pre-miR-7-transfected (*closed bars*) AZ521 cells and Kato-III cells are shown (mean ± s.d.). *$p < 0.05$.

Figure 4. The mechanism responsible for the downregulation of miR-7 in gastric tumor cells. (a) Representative results of methylated (*top*) or unmethylated (*bottom*) status-specific PCR for miR-7-1. *Lanes 1-12,* human gastric cancer samples; *lanes 13-22*, non-tumor stomach samples; *lane 23*, methylated DNA control; *lane 24*, unmethylated DNA control; and *lane 25*, water control. (b) The results of ChIP-PCR analyses of miR-7-1 and the house-keeping genes, *Gapdh* and *Eef1a1*, for H3K27me3 in the gastric mucosa of respective genotype mice. The percentages of immunoprecipitated (*IP*)/whole cell extracts (*WCE*) are shown for each primer set. (c) The luciferase activities of miR-7 Luc- or control Luc-transfected AZ521 reporter cells stimulated with CM(+) (*gray bars*) relative to those with CM(-) (*open bars*) are shown (mean ± s.d.). *$p < 0.05$. Conditioned medium was prepared from RAW264 cells (*left*) or intraperitoneal macrophages (*right*). (d) The luciferase activities of miR-7 Luc-transfected AZ521 reporter cells stimulated with whole CM(+) (*closed bars*), CM(+) fractionated to the indicated molecular sizes (*gray bars*), or fractionated CM(+) to < 3kDa collected from celecoxib-treated and LPS-stimulated macrophages (*light gray bar*) relative to the control level (*open bar*) are shown (mean ± s.d.). *$p < 0.05$ versus the control level. (e) The relative miR-7 expression levels examined by real-time RT-PCR in AZ521 cells stimulated

with whole CM(+) or fractioned CM(+) < 3 kDa relative to the control level are shown (mean ± s.d.). *$p < 0.05$ versus the control level. The expression levels of miR-7 were normalized to the U44 level.

Figure 5. The inflammation-induced miR-7 expression in the mouse stomachs. (a) Histology of the wild-type mouse normal glandular stomach (*top*) and *H. felis*-infected inflamed glandular stomach (*bottom*). Arrows and inset indicate submucosal inflammatory cell infiltration. Scale bars indicate 0.5 mm. (b) Immunostaining of F4/80 in the normal glandular stomach (*top*) and *H. felis*-infected glandular stomach (*bottom*). Arrowheads indicate macrophages. Scale bars indicate 100 μm. (c) The miR-7 expression level of *H. felis*-infected gastric mucosa (*gray bar*) relative to that of the control stomach (*open bar*) is shown (mean ± s.d.). *$p < 0.05$. (d) Immunostaining of F4/80 in a SPF control *Gan* mouse tumor (*top*) and a germfree *Gan* mouse tumor (*bottom*). Arrowheads indicate macrophages. Scale bars indicate 100 μm. (e) The expression levels of miR-7 in SPF (*gray bars*) and germfree (*closed bars*) *K19-C2mE* mouse gastritis and *Gan* mouse gastric tumors relative to the SPF wild-type stomach levels are shown (mean ± s.d.). *$p < 0.05$. The expression levels of miR-7 were normalized to the Sno202 level.

Figure 6. Inflammation-dependent upregulation of miR-7 target genes. (a) Representative results of the Western blotting analysis of EGFR in Kato-III cells (*top left*) and AZ521 cells (*top right*) transfected with pre-miR-NC and pre-miR-7. The results for

two independently prepared samples are shown. β-Actin was used as an internal control. The relative band intensities of the Western blotting results are shown in the bar graph (mean ± s.d.) (*bottom*). *$p < 0.05$ versus the control level. (b) The alignment of the miR-7 target sequences in the 3'-UTR of *Lphn2*, *Basp1*, and *Mafg* in human and mouse mRNAs. The seed match sequences for miR-7 are indicated in red. (c) The expression levels of the indicated genes in *K19-C2mE* mouse gastritis (*green bars*), *Gan* mouse gastric tumors (*yellow bars*), and *K19-Nog/C2mE* mouse gastric hamartomas (*blue bars*) relative to the wild-type levels (*gray bars*) are shown (mean ± s.d.). *$p < 0.05$ versus the wild-type level. The results were extracted from the microarray data set (Gene Expression Omnibus (GEO), accession GSE16902). (d) The expression levels of the indicated genes examined by real-time RT-PCR in the pre-miR-7-transfected Kato-III cells (*closed bar*) relative to those of the control cells (*gray bar*) are shown (mean ± s.d.). *$p < 0.05$ versus control level. (e) The relative luciferase activity levels of pre-miR-7-transfected reporter cells (*closed bars*) to the levels of control pre-miR-NC-transfected reporter cells (*gray bars*) are shown. The target genes for the respective luciferase reporter vectors are indicated. *$p < 0.05$ versus the control level. (f) Comparison of the relative expression levels of miR-7 and *LPHN2* (*left*), *BASP1* (*center*) or *MAFG* (*right*) in human gastric cancers to the non-tumor stomach levels is shown. Red and blue lines indicate that miR-7 was increased (>1.0) and decreased (< 1.0) in gastric cancers, respectively. The expression levels of miR-7 were normalized to the U44 level.

Figure 1

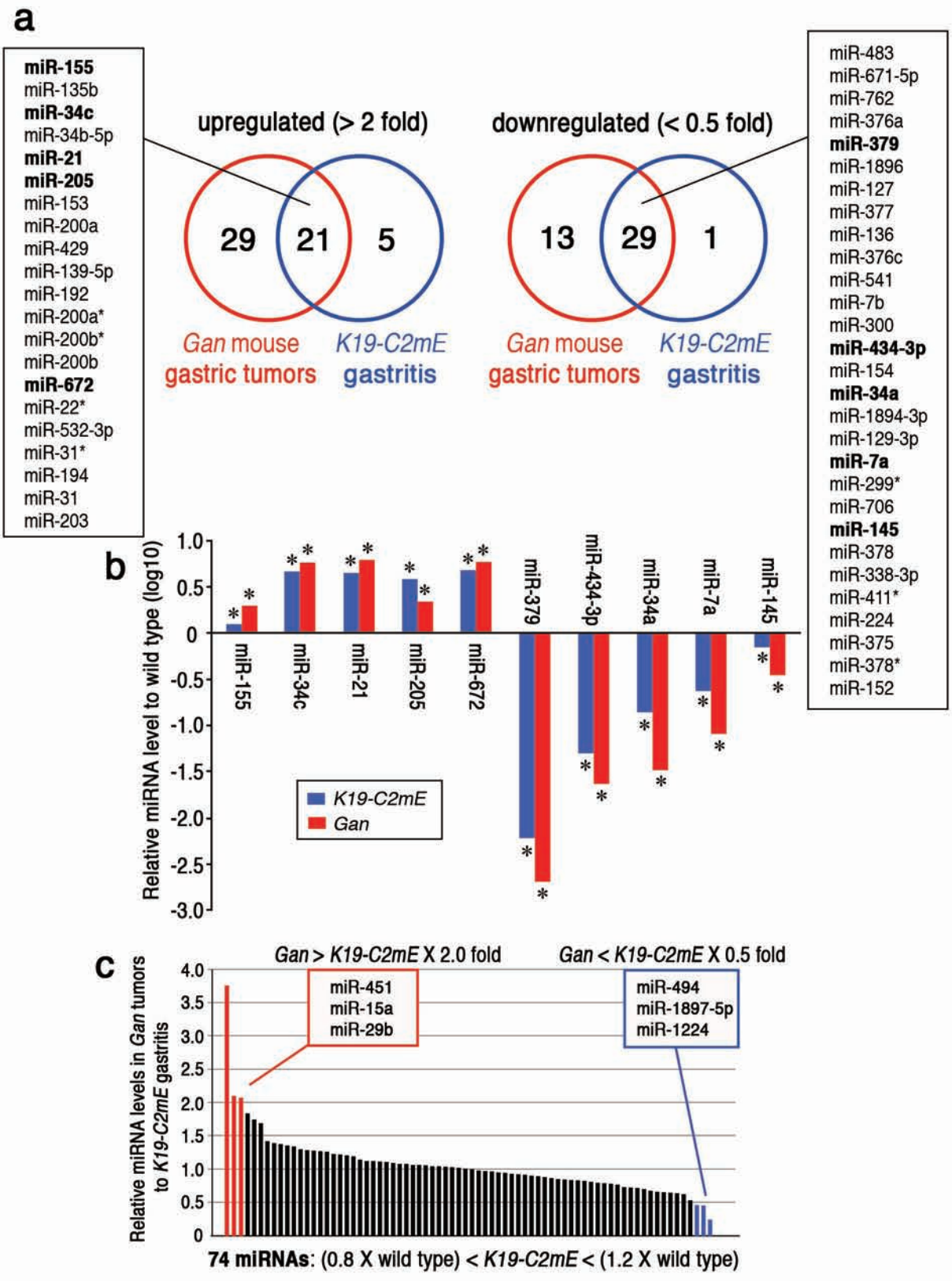
a
miR-155
miR-135b
miR-34c
miR-34b-5p
miR-21
miR-205
miR-153
miR-200a
miR-429
miR-139-5p
miR-192
miR-200a*
miR-200b*
miR-200b
miR-672
miR-22*
miR-532-3p
miR-31*
miR-194
miR-31
miR-203
upregulated (> 2 fold)
29
21
5
Gan mouse gastric tumors
K19-C2mE gastritis
downregulated (< 0.5 fold)
13
29
1
Gan mouse gastric tumors
K19-C2mE gastritis
miR-483
miR-671-5p
miR-762
miR-376a
miR-379
miR-1896
miR-127
miR-377
miR-136
miR-376c
miR-541
miR-7b
miR-300
miR-434-3p
miR-154
miR-34a
miR-1894-3p
miR-129-3p
miR-7a
miR-299*
miR-706
miR-145
miR-378
miR-338-3p
miR-411*
miR-224
miR-375
miR-378*
miR-152
b
Relative miRNA level to wild type (log10)
1.0
0.5
0
-0.5
-1.0
-1.5
-2.0
-2.5
-3.0
miR-155
miR-34c
miR-21
miR-205
miR-672
miR-379
miR-434-3p
miR-34a
miR-7a
miR-145
K19-C2mE
Gan
c
Gan > K19-C2mE X 2.0 fold
Gan < K19-C2mE X 0.5 fold
miR-451
miR-15a
miR-29b
miR-494
miR-1897-5p
miR-1224
Relative miRNA levels in Gan tumors to K19-C2mE gastritis
4.0
3.5
3.0
2.5
2.0
1.5
1.0
0.5
0
74 miRNAs: (0.8 X wild type) < K19-C2mE < (1.2 X wild type)

Figure 2

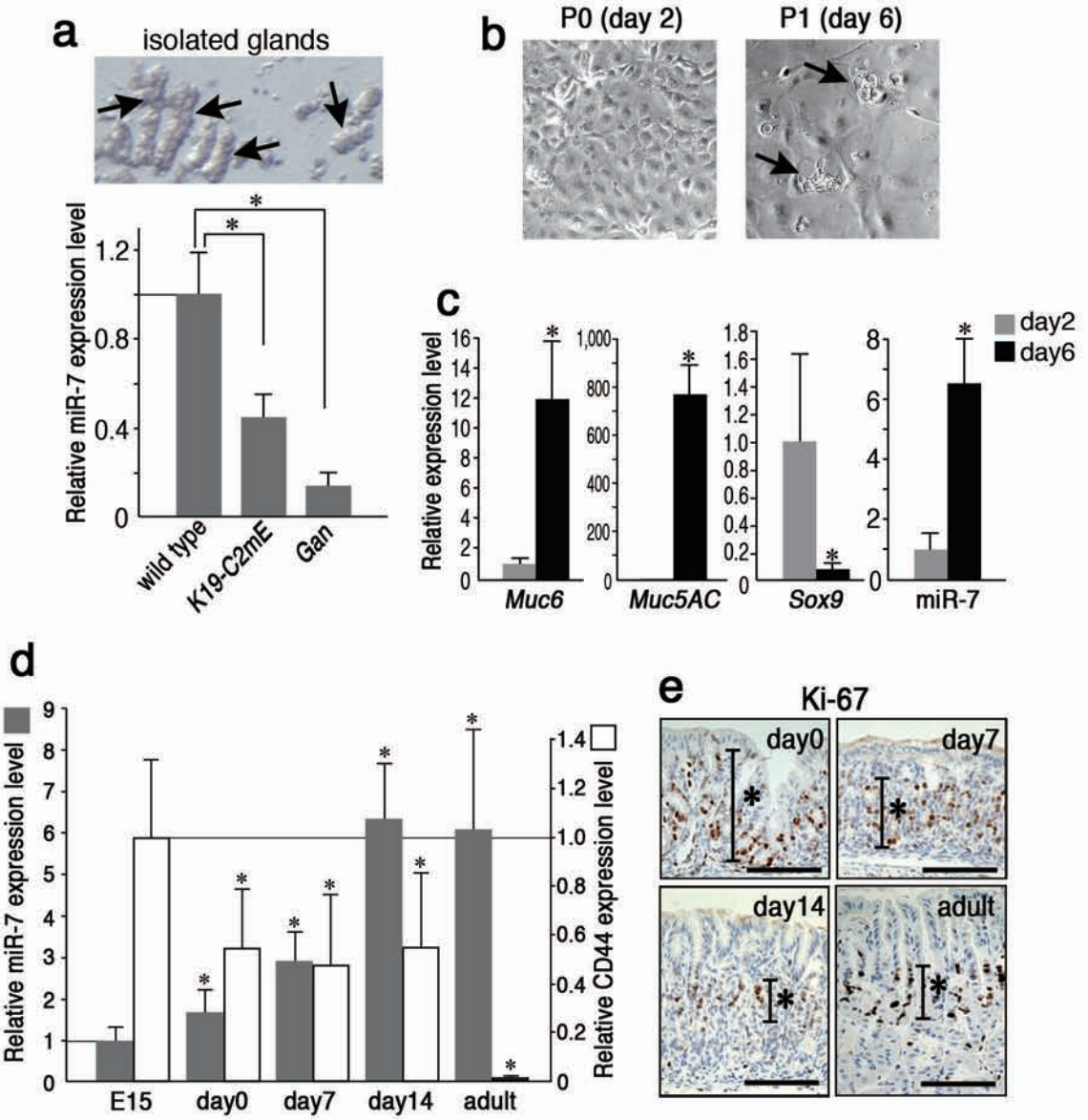
a
isolated glands
Relative miR-7 expression level
1.2
0.8
0.4
0
wild type
K19-C2mE
Gan
b
P0 (day 2)
P1 (day 6)
c
day2
day6
Relative expression level
Muc6
Muc5AC
Sox9
miR-7
d
Relative miR-7 expression level
Relative CD44 expression level
E15
day0
day7
day14
adult
e
Ki-67
day0
day7
day14
adult

Figure 3

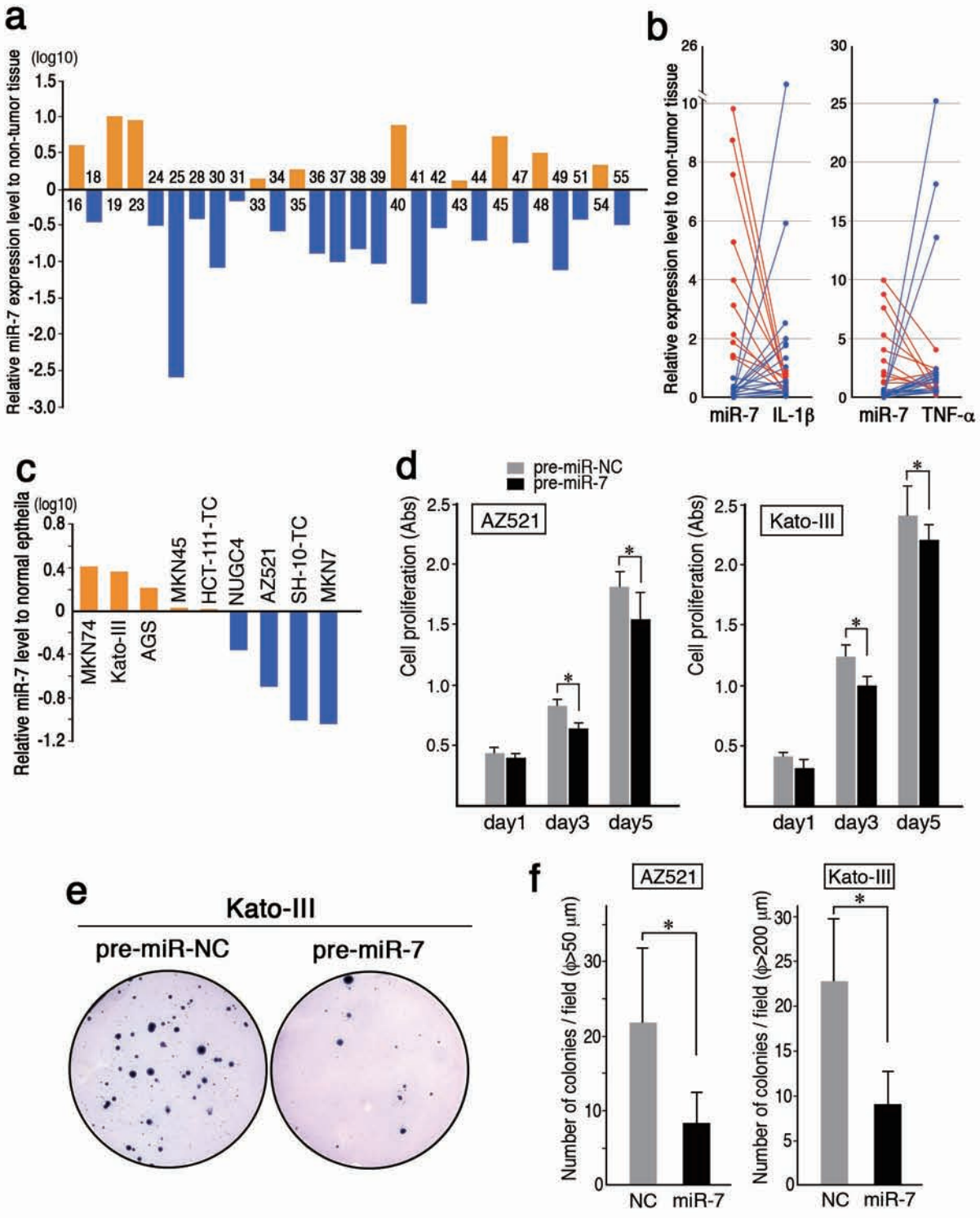
a
(log10)
Relative miR-7 expression level to non-tumor tissue
1.5
1.0
0.5
0
-0.5
-1.0
-1.5
-2.0
-2.5
-3.0
16 18 19 23 24 25 28 30 31 33 34 35 36 37 38 39 40 41 42 43 44 45 47 48 49 51 54 55
b
Relative expression level to non-tumor tissue
26
10
8
6
4
2
0
30
25
20
15
10
5
0
miR-7 IL-1β
miR-7 TNF-α
c
(log10)
Relative miR-7 level to normal epithelia
0.8
0.4
0
-0.4
-0.8
-1.2
MKN74
Kato-III
AGS
MKN45
HCT-111-TC
NUGC4
AZ521
SH-10-TC
MKN7
d
pre-miR-NC
pre-miR-7
AZ521
Kato-III
Cell proliferation (Abs)
2.5
2.0
1.5
1.0
0.5
day1 day3 day5
*
e
Kato-III
pre-miR-NC
pre-miR-7
f
AZ521
Kato-III
Number of colonies / field (ϕ>50 μm)
Number of colonies / field (ϕ>200 μm)
30
20
10
0
NC miR-7
*

Figure 4

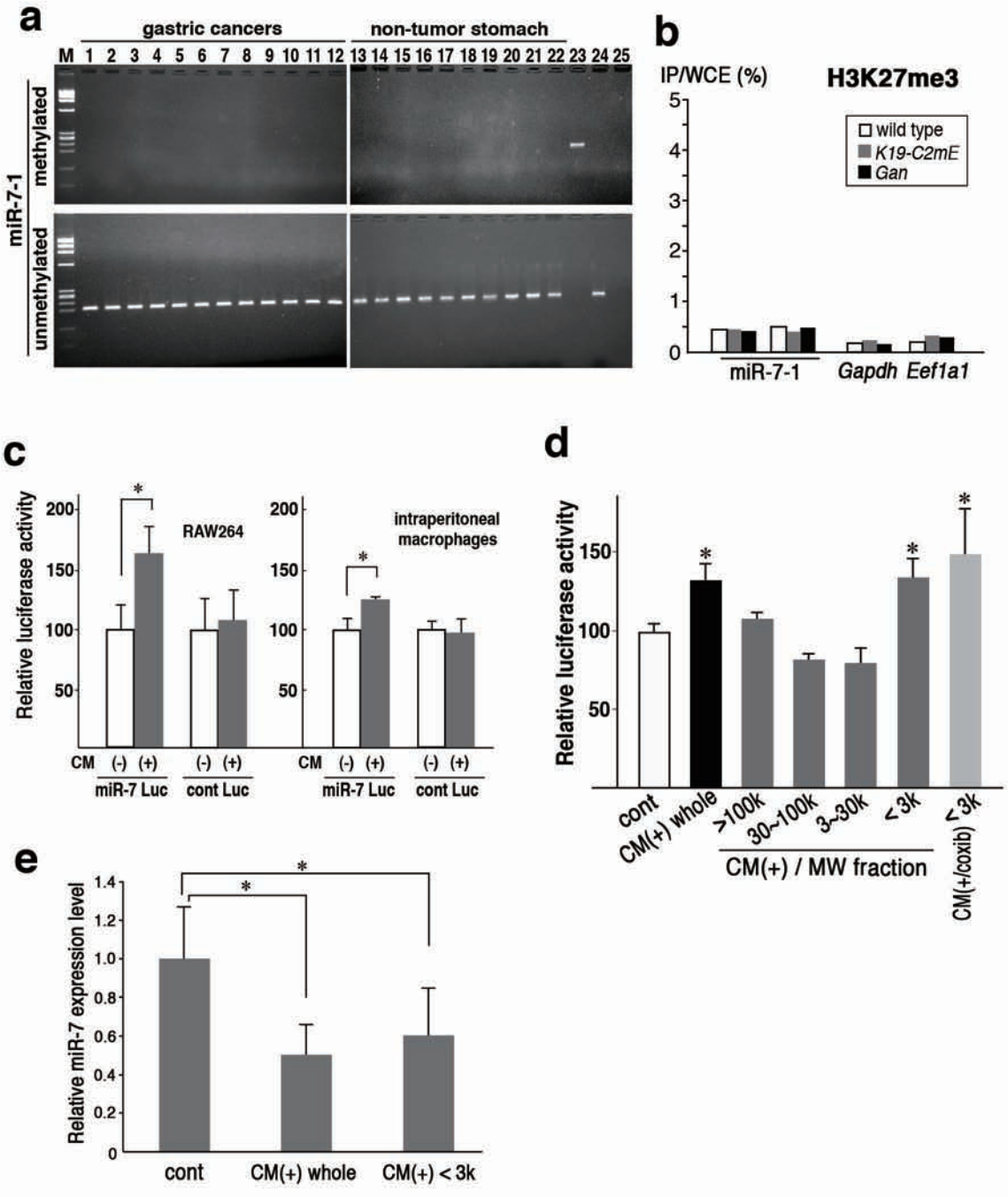
a
gastric cancers
non-tumor stomach
M 1 2 3 4 5 6 7 8 9 10 11 12 13 14 15 16 17 18 19 20 21 22 23 24 25
miR-7-1
methylated
unmethylated
b
IP/WCE (%)
H3K27me3
wild type
K19-C2mE
Gan
miR-7-1
Gapdh
Eef1a1
c
Relative luciferase activity
RAW264
intraperitoneal macrophages
CM (-) (+) (-) (+)
miR-7 Luc
cont Luc
d
Relative luciferase activity
cont
CM(+) whole
>100k
30~100k
3~30k
<3k
CM(+/coxib)
CM(+) / MW fraction
e
Relative miR-7 expression level
cont
CM(+) whole
CM(+) < 3k

Figure 5

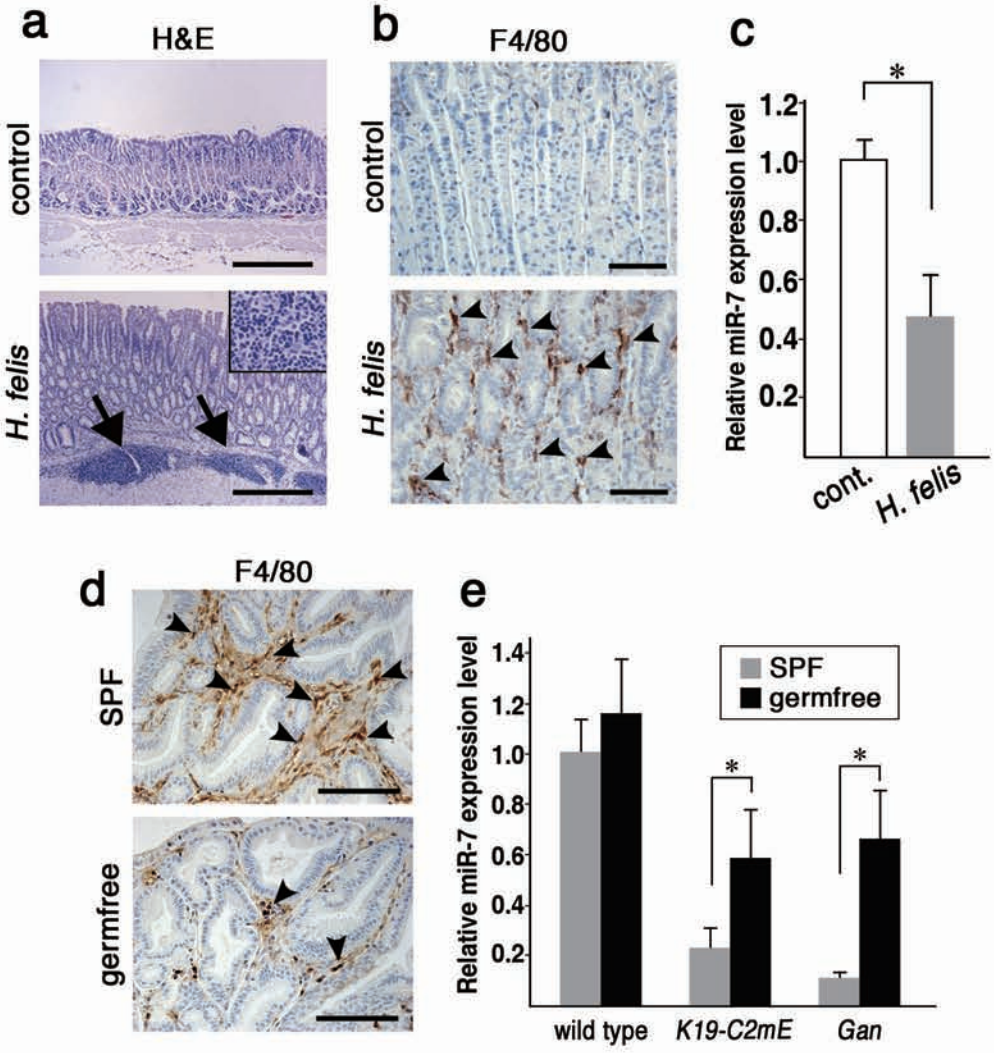
a
H&E
control
H. felis
b
F4/80
control
H. felis
c
Relative miR-7 expression level
1.2
1.0
0.8
0.6
0.4
0.2
*
cont.
H. felis
d
F4/80
SPF
germfree
e
Relative miR-7 expression level
1.4
1.2
1.0
0.8
0.6
0.4
0.2
SPF
germfree
*
*
wild type
K19-C2mE
Gan

Figure 6

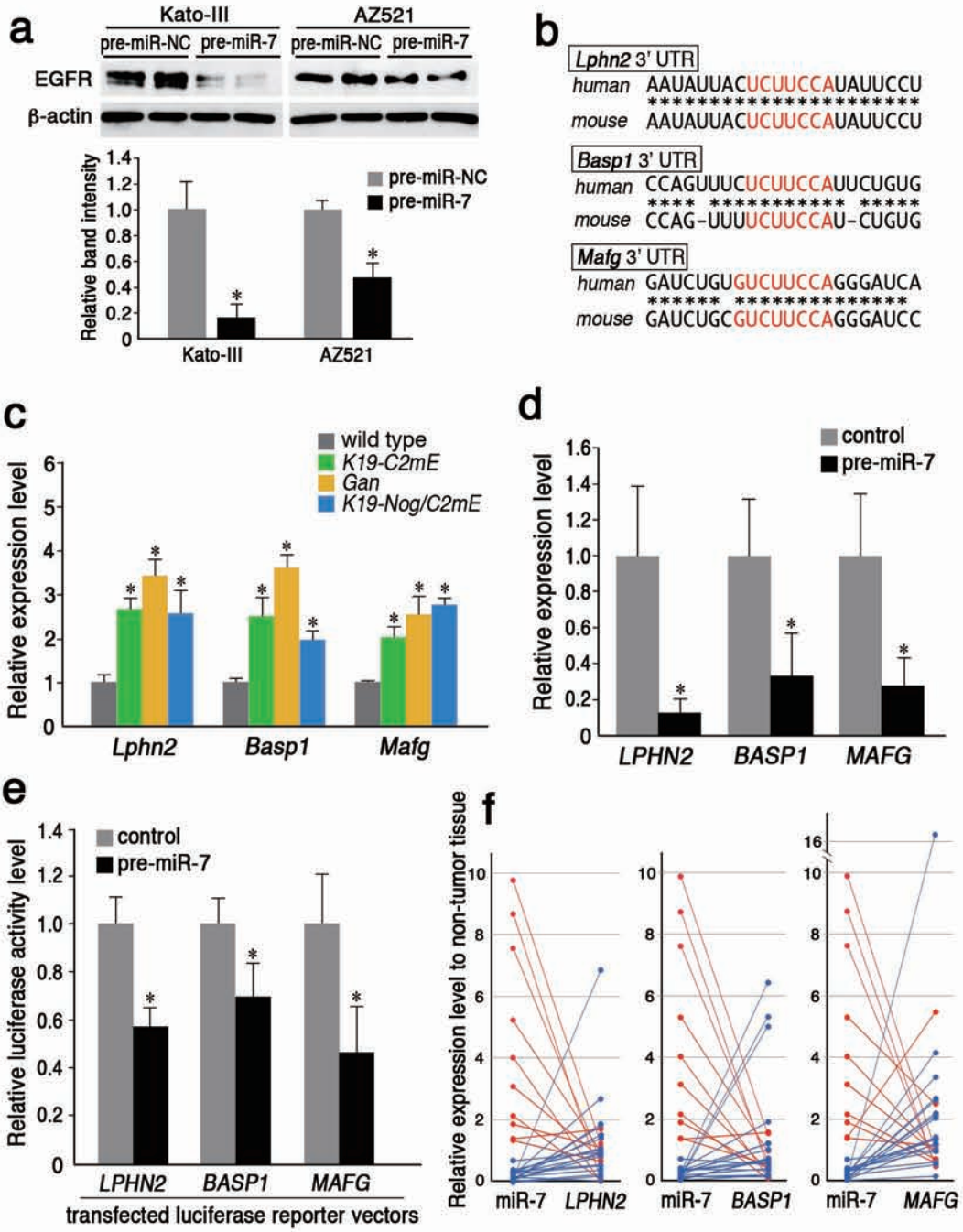
a
Kato-III
AZ521
pre-miR-NC
pre-miR-7
pre-miR-NC
pre-miR-7
EGFR
β-actin
Relative band intensity
pre-miR-NC
pre-miR-7
Kato-III
AZ521
b
Lphn2 3' UTR
human AAUAUUACUCUUCCAUAUUCCU
mouse AAUAUUACUCUUCCAUAUUCCU
Basp1 3' UTR
human CCAGUUUCUCUUCCAUUCUGUG
mouse CCAG-UUUUCUUCCAU-CUGUG
Mafg 3' UTR
human GAUCUGUGUCUUCCAGGGAUCA
mouse GAUCUGCGUCUUCCAGGGAUCC
c
Relative expression level
wild type
K19-C2mE
Gan
K19-Nog/C2mE
Lphn2
Basp1
Mafg
d
Relative expression level
control
pre-miR-7
LPHN2
BASP1
MAFG
e
Relative luciferase activity level
control
pre-miR-7
LPHN2
BASP1
MAFG
transfected luciferase reporter vectors
f
Relative expression level to non-tumor tissue
miR-7
LPHN2
miR-7
BASP1
miR-7
MAFG